Journal of Thermal Analysis and Calorimetry (2020) 141:739–749
https://doi.org/10.1007/s10973-019-09082-y

Microcalorimetric evaluation of the effects of three anthraquinone derivatives from Chinese Rhubarb and the synergistic effect of the mixture on *Staphylococcus aureus*

Xiangka Hu[1] · Yue Ma[1] · Zuodong Liu[1] · Miaoxin Zhao[1] · Sumin Dong[1] · He Yang[1] · Chunmei Dai[1]

Received: 18 June 2019 / Accepted: 18 November 2019 / Published online: 27 November 2019

Abstract
In this study, a noninvasive and nondestructive microcalorimetric method was used to investigate the antimicrobial activity of three anthraquinone derivatives (emodin, aloe-emodin and physcion) from Chinese Rhubarb. Additionally, we observed a synergistic antibacterial effect of a mixture (emodin + aloe-emodin) on *Staphylococcus aureus*. Antibacterial effects were further evaluated through principle component analysis and the half-inhibitory concentration (IC_{50}) according to the influence of the anthraquinone derivatives on eight quantitative thermokinetic parameters, which were measured by isothermal microcalorimetry and obtained from metabolic power–time curves of *Staphylococcus aureus* growth at 37 °C. The inhibitory actions of the anthraquinone derivatives varied at different concentrations. The antibacterial effect of the derivatives on *S. aureus* was as follows: emodin + aloe-emodin (E + AE) > emodin (E) > aloe-emodin (AE) > physcion. Based on these results, the combined effect of emodin and aloe-emodin was stronger than that of each anthraquinone derivative alone. The combination of emodin and aloe-emodin is a promising antibacterial agent, providing a novel avenue for antibacterial materials.

Keywords Emodin · Aloe-emodin · Physcion · Antibacterial · Synergistic · *S. aureus*

Introduction

Staphylococcus aureus, a gram-positive commensal bacterium, is a major human pathogen that can cause serious clinical infections, including bacteraemia and skin, soft tissue and device-related infections [1]. *S. aureus* can also enter the bloodstream, further endangering health [2]. Seven different pore-forming protein toxins produced by *S. aureus* promote disease, and antibiotic-resistant *S. aureus* is closely related to high morbidity and mortality in nosocomial infections involving severe sepsis and septic shock [3]. As toxicity and antibiotic resistance have rendered current drugs ineffective, it is necessary to develop antibacterial agents with high efficacy and low toxicity [4].

Drugs that inhibit the growth of pathogenic microorganisms or kill them without damaging host cells are considered promising candidates. Anthraquinone derivatives from Chinese Rhubarb possess extensive pharmacological properties, including anti-inflammatory [5–7], antiproliferation [8, 9], anticancer [5, 10, 11], antioxidant [12], hepatoprotective [13, 14] and antibacterial effects [5, 15]. The major active components of anthraquinone derivatives are emodin, aloe-emodin and physcion, and numerous studies have focussed on the individual pharmacological effects of these compounds [16–18]. Conversely, synergistic effects of anthraquinone derivatives (emodin and aloe-emodin) have attracted little attention. In addition, traditional Chinese medicine tends to separate and analyze the active components or effective monomers of Chinese herbal medicine while neglecting combined effects. Thus, synergistic effect among active ingredients (e.g., emodin and aloe-emodin) is worthy of study.

Microcalorimetry, which is noninvasive and nondestructive, can be employed to analyze overall dynamic changes in microbial growth and has been well applied in modern medical research [19, 20]. Compared to conventional microbiological methods (e.g., microplate, turbidimetry assays, the disk diffusion method), microcalorimetry can provide important qualitative and quantitative information in real time, online and high-throughput screening assays [21–24]. With good sensitivity, accuracy and reproducibility, this approach has been widely used to discover new drugs and evaluate antibacterial activity [21].

✉ Chunmei Dai
lnmupharmacy@163.com

[1] Jinzhou Medical University, Jinzhou 121000, China

Based on the above advantages, the microcalorimetric method was used to evaluate the antibacterial effects of emodin, aloe-emodin and physcion alone as well as the synergistic inhibitory effect of emodin and aloe-emodin on the growth of *S. aureus*. The aims of this study were to (1) objectively and effectively assess the individual antibacterial effects of emodin, aloe-emodin and physcion, and the synergistic effect of emodin and aloe-emodin, (2) provide helpful references to gain a better understanding of the activities of anthraquinone derivatives on microorganisms and (3) provide a novel method for screening new antibacterial drugs with high efficacy and low toxicity.

Materials and methods

Materials

S. aureus (CMCC B26003) was purchased from the China Center for Type Culture Collection and inoculated in Luria–Bertani (L.B.) culture medium (L.B. medium: 10 g peptone, 5 g yeast extract and 5 g NaCl per 1000 mL distilled water, pH 7.2–7.4). The culture medium was pre-sterilized using high-pressure (0.1 MPa) steam at 121 °C for 30 min and stored at 4 °C before use.

Preparation of samples

Emodin, aloe-emodin and physcion (purity: ≥98%, HPLC) were purchased from the Tianjin Jianfeng Natural Product Center; their structures are shown in Fig. 1. Because of the poor water solubility of anthraquinone derivatives, emodin, aloe-emodin and physcion were dissolved in dimethylsulfoxide (DMSO; Sigma) at 20 mg mL^{-1} as stock solutions. The stock solutions were stored at −20 °C and protected from light [25]. Repeated preliminary experiments showed that the influence of 25 μL DMSO in 5 mL *S. aureus* suspension was negligible. Thus, for this experiment, the final proportion of DMSO in the *S. aureus* suspension was below 0.5% (v/v) [6, 25, 26].

Instrumentation

A TAM Air isothermal microcalorimeter (Thermometric AB, Sweden) was used to record metabolic power–time curves of *S. aureus* growth. This microcalorimeter is an eight-channel twin instrument with a limit of detection of 2 μW and a baseline draft < 20 μW over 24 h, which maintains the temperature within ±0.02 °C. The eight channels are fixed together to form a single heat-sink block placed in a temperature-controlled air thermostat. Each calorimetric channel consists of two parts: one for the sample and another as a static reference. The two parts within a channel allow direct comparison of the heat-output power from the sample with that from the static reference. The power difference is a quantitative expression of the overall rates of heat production in the samples. The temperature was controlled at 37 °C for all experiments [4, 27]. Additional information regarding the TAM air has been reported by Wadsö [28].

Experimental procedure

In this calorimetric experiment, metabolic power–time curves of *S. aureus* growth were recorded using the isothermal calorimeter with the ampoule method. *S. aureus* was inoculated into 45 mL of L.B. culture medium at an initial density of 2×10^6 colony-forming units (CFU) per mL. Then, 5 mL of bacterial suspension was added to sterilized 20-mL glass ampoules. Emodin, aloe-emodin and physcion were added to the bacterial suspension at different concentrations. The ampoules were sealed, shaken slightly and placed in the microcalorimeter when a steady state was reached. After balancing the instrument, the heat flow power–time curves of *S. aureus* growth were recorded by a computer. Records were obtained by the TAM air software until the recorder returned to baseline. In all experiments, the temperature was controlled at 37 °C. Emodin and aloe-emodin (1:8, W/W) were mixed and tested according to the above steps. The above experiments were all performed under aseptic conditions [29].

Results

Metabolic power–time curves and growth rate constant of *S. aureus*

The metabolic power–time curve of *S. aureus* growth at 37 °C in the absence of samples is shown in Fig. 2a. As *S. aureus* was inoculated in L.B. culture medium under

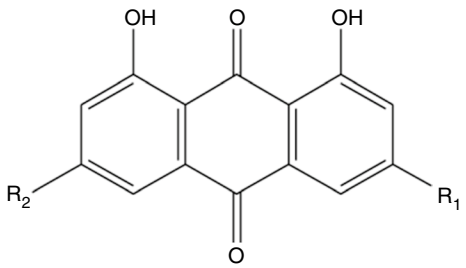

	R_1	R_2
emodin	OH	CH_3
aloe–emodin	CH_2OH	H
physcion	OCH_3	CH_3

Fig. 1 Chemical structure of emodin, aloe-emodin and physcion extracted from Chinese Rhubarb

isochoric conditions and limited nutrients and oxygen, the observable growth curve of *S. aureus* consisted of two stages (stage 1 and stage 2) and five phases [lag phase (a–b), first exponential phase (b–c), transition phase (c–d), second exponential phase (d–e) and decline phase (e–f)] [21, 27, 29]. The quantitative thermokinetic parameters (growth rate constant k) of the power–time curve for *S. aureus* growth were obtained from Eq. (1):

$$P_t = P_0 \exp(kt) \text{ or } \ln P_t = \ln P_0 + kt \quad (1)$$

where P_0 and P_t represent the heat-output power at time $t=0$ and time t (min), respectively. The growth rate constant k of the exponential phase was calculated by fitting $\ln P_t$ and t to a linear equation. The values of k_1 and k_2 with the corresponding RSDs of 0.82% and 1.07% are shown in Table 1, which indicated a good reproducibility of the experiments.

Metabolic power–time curves of *S. aureus* growth affected by anthraquinone derivatives

As presented in Fig. 2b, as the concentration of emodin increased, the heights of the highest peak for *S. aureus* in stage 2 decreased, the corresponding peak time lengthened; and the heights and peak time of the highest peak for *S. aureus* in stage 1 increased slightly.

Figure 2c illustrated that as the concentration of aloe-emodin increased, the heights of the highest peak for *S. aureus* in stage 2 and stage 1 were reduced, but that the corresponding peak time was prolonged.

According to Fig. 2d, when the concentration of physcion increased, the heights and peak time of the highest peak for *S. aureus* in stage 1 were almost unchanged, and the heights and peak time of the highest peak for *S. aureus* in stage 2 decreased.

Lastly, Fig. 2e illustrated that the heights of the highest peak for *S. aureus* affected by AE + E (emodin and aloe-emodin) decreased, but that the corresponding peak time increased in stage 2. The heights and peak time of the highest peak for *S. aureus* affected by emodin in stage 1 were almost unaltered. The heights of the highest peak for *S. aureus* affected by AE + E and aloe-emodin in stage 1 were reduced, and the corresponding peak time increased. In addition, the changes in the power–time curves for *S. aureus* growth affected by AE + E and aloe-emodin in stage 1 were almost identical.

Thermokinetic parameters of metabolic power–time curves for *S. aureus* growth affected by anthraquinone derivatives

Eight quantitative thermokinetic parameters were obtained from the metabolic power–time curves of *S. aureus* affected by anthraquinone derivatives, as given in Tables 2–5. The k_1 and k_2 parameters are the growth rate constants of the first and second exponential phases, respectively. P_1 and P_2 are the maximum heat-output powers of the first and second peaks, respectively, and t_1 and t_2 are the appearance times of P_1 and P_2, respectively. Q_1 and Q_2 are the heat outputs at stages 1 and 2, respectively.

The data in Tables 2–5 demonstrated that the eight metabolic thermokinetic parameters had variable changing trends depending on the anthraquinone derivative concentration and species. As shown in Table 2, compared with the control, k_2, P_2 and Q_2 decreased and t_2 increased markedly as the concentration of emodin increased. Additionally, k_1 decreased, and P_1 increased, but both changes were small; t_1 and Q_1 exhibited almost no change. The results suggested that the inhibitory effect of emodin on *S. aureus* was enhanced by an increasing concentration and had an important effect in stage 2, consistent with the data in Fig. 2b.

As shown in Table 3, when the concentration of aloe-emodin increased, the values of k_1, k_2, P_1, P_2, Q_1 and Q_2 decreased and those of t_1 and t_2 increased compared with the control. These results indicate that aloe-emodin had an inhibitory effect on *S. aureus* at both stage 1 and stage 2, consistent with Fig. 2c.

The values of k_1, P_1, t_1 and Q_1 showed almost no change compared with the control, but the values of k_2 and Q_2 decreased slightly (see Table 4). However, P_2 decreased slightly when $c > 10$ μg.mL^{-1}, and t_2 decreased slightly when $c > 30$ μg.mL^{-1}. These data showed that physcion exerted very little bacteriostatic activity toward *S. aureus*, which was consistent with Fig. 2d.

According to the data presented in Table 5, the values of k_2, P_1 and P_2 of *S. aureus* affected by AE + E were the smallest. k_1 of *S. aureus* affected by AE + E was almost the same as that affected by AE, but was smaller than that affected by E. The results showed that the synergistic antibacterial effect of emodin and aloe-emodin on *S. aureus* appeared to be the strongest in stage 2, with an impact in stage 1. This is more understandable when combined with those in Fig. 2e.

The thermokinetic parameters of *S. aureus* growth varied with different anthraquinone derivative concentrations and species, exhibiting the same effective trend as the metabolic power–time curves of *S. aureus* affected by anthraquinone derivatives (Fig. 2). In other words, smaller values of k_1, k_2, P_1, P_2, Q_1 and Q_2 and larger values of t_1 and t_2 correlated with stronger bacteriostatic activity of anthraquinone derivatives.

Principal component analysis of eight thermokinetic parameters

Principal component analysis (PCA) is based on dimension reduction, a statistical method that transforms a number of interrelated numerical variables into a few unrelated

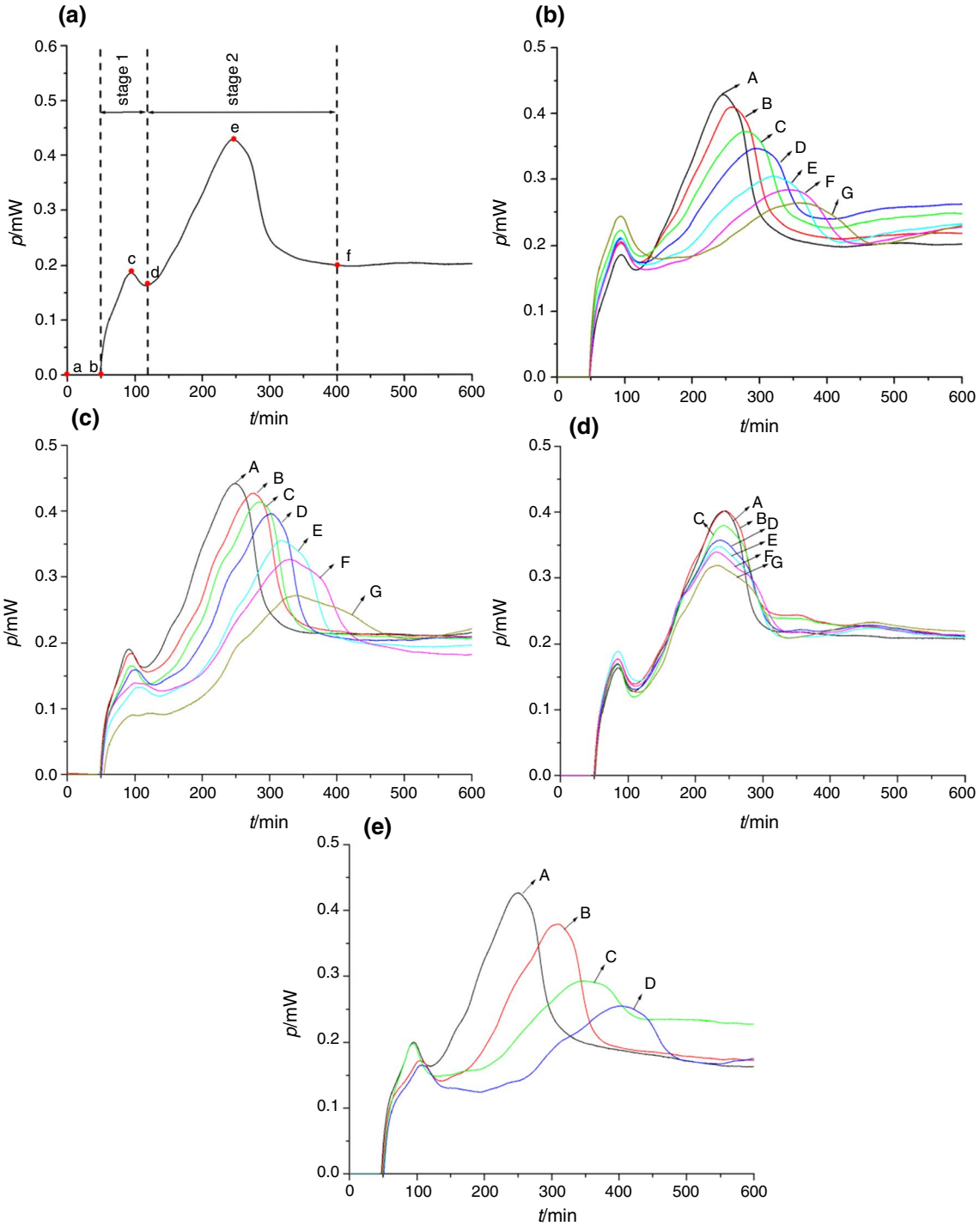

Fig. 2 Metabolic power–time curves of *S. aureus* growth **a** without anthraquinone derivatives and affected by different concentrations of **b** emodin [(A) control, (B) 0.2 μg mL^{-1}, (C) 0.4 μg mL^{-1}, (D) 0.6 μg mL^{-1}, (E) 0.8 μg mL^{-1}, (F) 1.0 μg mL^{-1}, (G) 1.2 μg mL^{-1}]; **c** aloe-emodin [(A) control, (B) 1.2 μg mL^{-1}, (C) 2.4 μg mL^{-1}, (D) 4.8 μg mL^{-1}, (E) 9.6 μg mL^{-1}, (F) 19.2 μg mL^{-1}, (G) 38.4 μg mL^{-1}], **d** physcion [(A) control, (B) 10 μg mL^{-1}, (C) 30 μg mL^{-1}, (D) 50 μg mL^{-1}, (E) 70 μg mL^{-1}, (F) 90 μg mL^{-1}, (G) 100 μg mL^{-1}], and **e** two anthraquinone derivatives (E, AE) and their mixtures (0.8 μg mL^{-1} E + 6.4 μg mL^{-1} AE) [(A) control, (B) 6.4 μg mL^{-1} AE, (C) 0.8 μg mL^{-1} E, (D) 0.8 μg mL^{-1} E + 6.4 μg mL^{-1} AE]

Table 1 Growth rate constant k_1 and k_2 of *S. aureus* cultured in LB culture medium and monitored by the microcalorimeter at 37 °C

No.	1	2	3	4	5	6	7	8	RSD%[a]
k_1	0.0221	0.0224	0.0222	0.022	0.0223	0.0222	0.0225	0.0225	0.83
k_2	0.0079	0.0078	0.0077	0.0079	0.0077	0.0078	0.0078	0.0079	1.06

[a]Relative standard deviation

Table 2 The thermokinetic parameters of *S. aureus* growth affected by different concentrations of emodin and the corresponding inhibitory ratio *I*

C/μg.mL^{-1}	k_1/min^{-1}	k_2/min^{-1}	P_1/mW	P_2/mW	t_1/min	t_2/min	Q_1/J	Q_2/J	I/%
0	0.0255	0.0089	0.1861	0.4289	94.17	245.99	0.1158	1.6046	
0.2	0.0188	0.0071	0.2040	0.4095	94.17	256.61	0.1165	1.4071	20.22
0.4	0.0164	0.0057	0.2229	0.3726	93.04	279.54	0.1192	1.2035	35.96
0.6	0.0197	0.005	0.2106	0.3470	94.36	294.71	0.1164	1.0726	43.82
0.8	0.0196	0.0044	0.2121	0.3046	93.41	322.66	0.1172	0.9472	50.56
1.0	0.0197	0.0037	0.2063	0.2841	93.98	345.88	0.1164	0.8681	58.43
1.2	0.0148	0.0029	0.2437	0.2641	93.89	359.05	0.1970	0.6292	67.42

Table 3 The thermokinetic parameters of *S. aureus* growth affected by different concentrations of aloe-emodin and the corresponding inhibitory ratio *I*

C/μg.mL^{-1}	k_1/min^{-1}	k_2/min^{-1}	P_1/mW	P_2/mW	t_1/min	t_2/min	Q_1/J	Q_2/J	I/%
0	0.0255	0.0096	0.1906	0.4413	91.32	248.62	0.1157	1.5930	
1.2	0.0189	0.0083	0.1838	0.4267	95.82	276.19	0.1102	1.5658	13.54
2.4	0.0183	0.0083	0.1653	0.4138	95.66	285.52	0.1055	1.5418	13.54
4.8	0.0158	0.0078	0.1592	0.3958	101.4	302.79	0.1035	1.5276	18.75
9.6	0.0123	0.0075	0.1324	0.3548	104.7	316.22	0.0962	1.5074	21.87
19.2	0.0098	0.0068	0.1392	0.3260	99.52	330.61	0.0882	1.4893	29.17
38.4	0.0096	0.0067	0.0904	0.2711	99.92	340.82	0.0765	1.3780	30.21

Table 4 The thermokinetic parameters of *S. aureus* growth affected by different concentrations of physcion and the corresponding inhibitory ratio *I*

C/μg.mL^{-1}	k_1/min^{-1}	k_2/min^{-1}	P_1/mW	P_2/mW	t_1/min	t_2/min	Q_1/J	Q_2/J	I/%
0	0.0256	0.0101	0.1636	0.4012	85.24	242.21	0.1129	1.3419	
10	0.0257	0.0100	0.1772	0.4018	84.71	244.14	0.1118	1.3102	0. 99
30	0.0256	0.0099	0.1699	0.3797	83.49	243.26	0.1168	1.2319	1.98
50	0.0257	0.0095	0.1691	0.3570	85.68	236.60	0.1094	1.2153	5.94
70	0.0257	0.0092	0.1885	0.3470	85.15	234.06	0.1118	1.1752	8.91
90	0.0256	0.0089	0.1776	0.3389	84.48	229.86	0.1113	1.1695	11.88
100	0.0258	0.0087	0.1708	0.3188	84.54	232.57	0.1130	1.0834	13.86

Table 5 The thermokinetic parameters of *S. aureus* growth affected by aloe-emodin, emodin and AE + E and the corresponding inhibitory ratio *I*

Sample	k_1/min^{-1}	k_2/min^{-1}	P_1/mW	P_2/mW	t_1/min	t_2/min	Q_1/J	Q_2/J	I/%
control	0.0175	0.0088	0.2000	0.4264	94.83	249.12	0.1152	1.5342	
AE[a]	0.0105	0.0071	0.1718	0.3786	102.75	308.65	0.1066	1.4077	19.32
E[b]	0.0178	0.0046	0.1983	0.2923	94.29	343.19	0.1397	0.6967	47.72
AE + E[c]	0.0109	0.0035	0.1652	0.2548	107.79	403.42	0.1163	0.8551	60.23

[a]6.4 μg.mL^{-1} aloe-emodin

[b]0.8 μg.mL^{-1} emodin

[c]The mixture of 6.4 μg.mL^{-1} aloe-emodin and 0.8 μg.mL^{-1} emodin

comprehensive indices that are the principal components of the original multiple variables. Each principal component is a linear combination of original variables.

PCA is also a common approach to data analysis, as it can simplify multivariate variables and allow for transformation of the information in the data set into a few principal

components, retaining the maximum possible variability, as well as reduce the dimensionality of the original data set [30]. As a result, PCA simplifies experimental data processing and highlights the main variations [29, 31–34].

One task of PCA is to compute the principal components. After the original variables were standardized, correlation matrices between the variables, eigenvalues and eigenvectors of the matrices were calculated. The eigenvalues were then arranged in order of decreasing size (Tables 6–8), and the corresponding principal components were calculated. Another step of PCA is to determine the number of principal components. There were two methods: one was the accumulative contribution rate, whereby the accumulative contribution rate of N principal components could retain the first N principal components when reaching a certain value (generally above 70%) (Tables 6–8); the other involved eigenvalues, whereby principal components with eigenvalues ≥ 1 were selected (Tables 6–8).

PCA was performed using SPSS 20.0 software for the eight thermokinetic parameters (t_1, t_2, k_1, k_2, P_1, P_2, Q_1 and Q_2). Two principal components (Z_1 and Z_2) accounted for 85.75% (emodin, Table 6), 96.52% (aloe-emodin, Table 7) and 78.24% (physcion, Table 8) of the total variance [35]. The equations of Z_{emodin1} and Z_{emodin2}, $Z_{\text{aloe-emodin1}}$ and $Z_{\text{aloe-emodin2}}$, $Z_{\text{physcion1}}$ and $Z_{\text{physcion2}}$ are as follows:

$$Z_{\text{emodin1}} = 0.144k_1 + 0.168k_2 - 0.158P_1 + 0.163P_2 + 0.054t_1 - 0.162t_2 - 0.128Q_1 + 0.171Q_2$$
$$Z_{\text{emodin2}} = 0.348k_1 - 0.112k_2 - 0.245P_1 - 0.214P_2 + 0.733t_1 + 0.238t_2 + 0.075Q_1 - 0.153Q_2$$
$$Z_{\text{aloe - emodin1}} = 0.146k_1 + 0.146k_2 - 0.096P_1 + 0.148P_2 - 0.110t_1 - 0.149t_2 + 0.149Q_1 + 0.145Q_2$$
$$Z_{\text{aloe - emodin2}} = -0.217k_1 - 0.168k_2 - 0.651P_1 + 0.122P_2 + 0.519t_1 + 0.140t_2 + 0.116Q_1 + 0.248Q_2$$
$$Z_{\text{physcion1}} = -0.138k_1 + 0.223k_2 - 0.106P_1 + 0.221P_2 - 0.037t_1 + 0.213t_2 + 0.094Q_1 + 0.211Q_2$$
$$Z_{\text{physcion2}} = 0.096k_1 + 0.082k_2 + 0.020P_1 + 0.102P_2 + 0.506t_1 - 0.010t_2 - 0.462Q_1 + 0.183Q_2$$

The component plot of PCA showed that emodin (Fig. 3a) and physcion (Fig. 3c) played a major role in stage 2 of *S. aureus* growth, and aloe-emodin (Fig. 3b) played a major

Table 6 Principal component analysis for the eight thermokinetic parameters of *S. aureus* growth affected by different concentrations of emodin (total variance explained)

Component	Initial eigenvalues			Extraction sums of squared loadings		
	Total	% of Variance	Cumulative %	Total	% of variance	Cumulative %
1	5.700	71.254	71.254	5.700	71.254	71.254
2	1.159	14.491	85.745	1.159	14.491	85.745
3	0.823	10.284	96.029			
4	0.293	3.662	99.690			
5	0.023	0.293	99.983			
6	0.001	0.017	100.000			
7	−1.119E−016	−1.399E−015	100.000			
8	−2.606E−016	−3.257E−015	100.000			

Extraction method: principal component analysis

Table 7 Principal component analysis for the eight thermokinetic parameters of *S. aureus* growth affected by different concentrations of aloe-emodin (total variance explained)

Component	Initial eigenvalues			Extraction sums of squared loadings		
	Total	% of variance	Cumulative %	Total	% of variance	Cumulative %
1	6.583	82.285	82.582	6.583	82.285	82.285
2	1.139	14.232	96.517	1.139	14.232	96.517
3	0.218	2.720	99.238			
4	0.050	0.630	99.867			
5	0.008	0.104	99.971			
6	0.002	0.029	100.000			
7	2.827E−016	3.534E−015	100.000			
8	−5.684E−016	−7.105E−015	100.000			

Extraction method: principal component analysis

Table 8 Principal component analysis for the eight thermokinetic parameters of *S. aureus* growth affected by different concentrations of physcion (total variance explained)

Component	Initial eigenvalues			Extraction sums of squared loadings		
	Total	% of variance	Cumulative %	Total	% of variance	Cumulative %
1	4.371	54.633	54.633	4.371	54.633	54.633
2	1.889	23.608	78.241	1.889	23.608	78.241
3	0.865	10.809	89.051			
4	0.730	9.129	98.180			
5	0.110	1.371	99.551			
6	0.036	0.449	100.000			
7	2.238E−016	2.798E−015	100.000			
8	1.197E−016	1.497E−015	100.000			

Extraction method: principal component analysis

role in stage 1 and in stage 2 of *S. aureus* growth, supporting the above results. And this may play a more important role in evaluating their antibacterial effects on *S. aureus*. Combined with the values of Tables 2–4, we were able to rapidly and clearly identify the action potency of emodin, aloe-emodin and physcion on *S. aureus*: their inhibitory

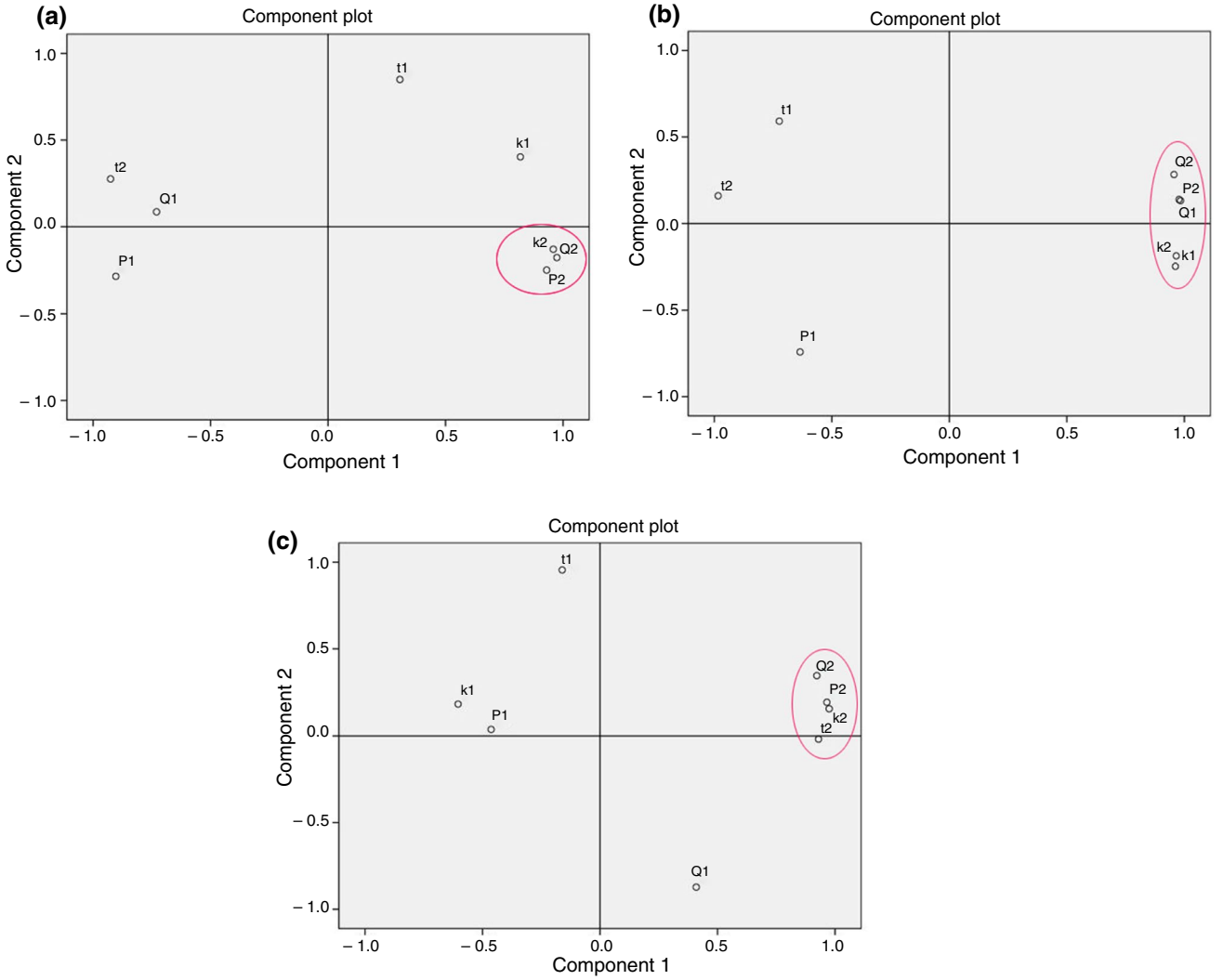

Fig. 3 Component plots of PCA for the eight thermokinetic parameters of *S. aureus* growth affected by different concentrations of **a** emodin, **b** aloe-emodin and **c** physcion

effect was stronger with increasing concentrations, consistent with Fig. 2b–d.

Inhibitory ratio *I* and half-inhibitory concentration IC_{50}

Based on the results of PCA, we chose k_2 to get the inhibitory ratio I by Eq. (2):

$$I = (k_{2c} - k_{2s}) / k_{2c} \times 100\% \quad (2)$$

where k_{2c} was the growth rate constant of the second exponential growth phase of *S. aureus* in the culture medium without anthraquinone derivatives and k_{2s} was the growth rate constant of the second exponential growth phase of *S. aureus* exposed to the anthraquinone derivatives. When the inhibitory ratio (I) was 50%, the corresponding concentration of the inhibitor could be observed to be the half-inhibitory concentration (IC_{50}), regarded as the inhibiting concentration causing a 50% decrease in the *S. aureus* growth rate constant [36].

We found that IC_{50} was approximately 0.8 μg.mL^{-1} for emodin, more than 38.4 μg.mL^{-1} for aloe-emodin and greater than 100 μg.mL^{-1} for physcion, as based on the linear relationship between k_2 and c from Fig. 4. In addition, when the *S. aureus* growth rate constant k_1 was 50%k_0, the corresponding concentration of aloe-emodin was approximately 6.4 μg.mL^{-1}. Thus, we selected 6.4 μg.mL^{-1} aloe-emodin combined with 0.8 μg.mL^{-1} emodin and assessed the synergistic inhibitory effect of this combination. As indicated in Fig. 2e and Table 5, the antibacterial effect of the anthraquinone derivatives was: AE + E > emodin > aloe-emodin > physcion. The values of I in Tables 4 and 5 also supported the above results.

Discussions

S. aureus can cause skin, soft tissue and bone infections, with a bloodstream infection being most serious [37]. Indeed, *S. aureus* present in the blood circulation results in higher mortality than any other bacterial infection [37].

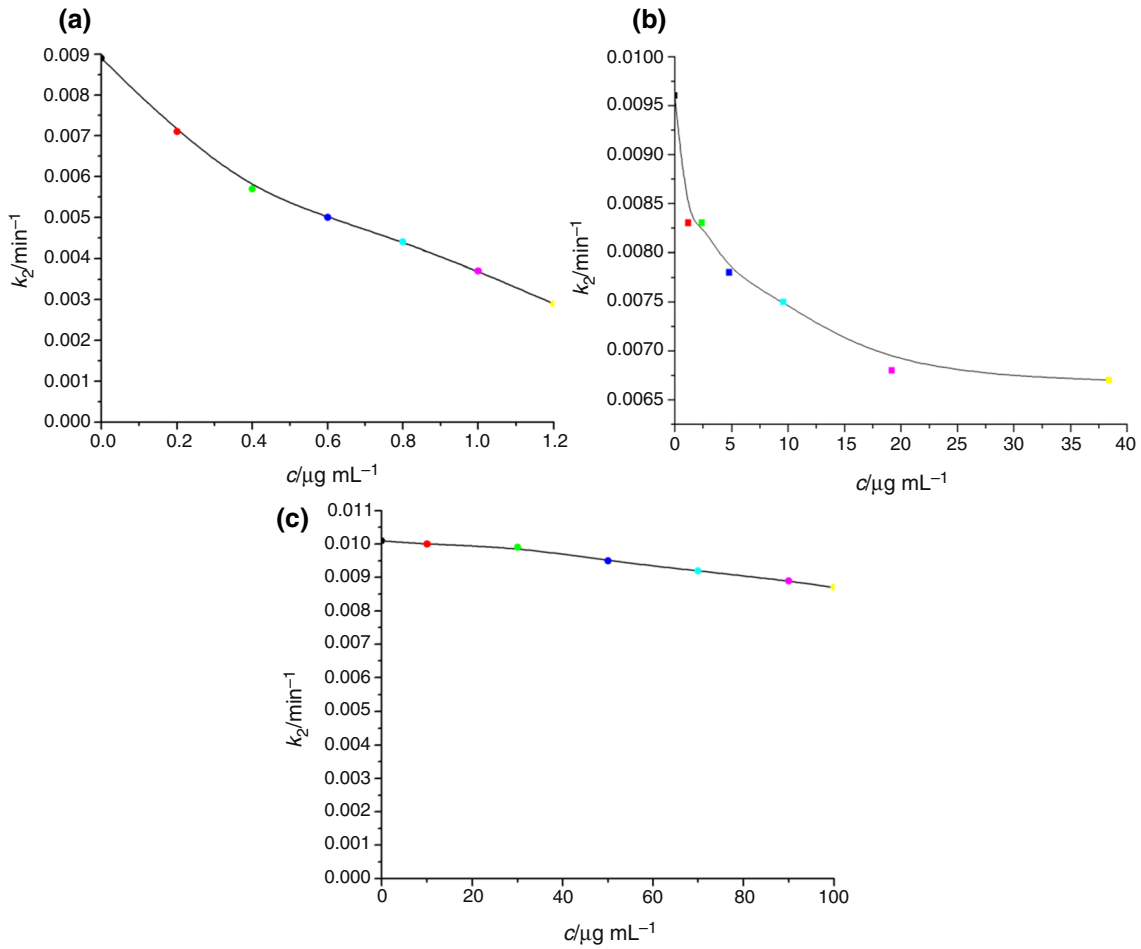

Fig. 4 Plots of k_2 of *S. aureus* growth versus concentration (c) of **a** emodin, **b** aloe-emodin and **c** physcion

Although numerous drugs have been assessed for their ability to control infection, *S. aureus* has developed resistance to almost all antibiotics [37–39]. Therefore, developing highly effective and low-toxicity agents against *S. aureus* has become highly urgent [40].

In this study, isothermal microcalorimetry was employed to evaluate the inhibitory effects of anthraquinone derivatives (emodin, aloe-emodin and physcion) and a mixture (emodin combined with aloe-emodin) on *S. aureus*. As seen from the results, we have known that the antimicrobial activity of physcion on *S. aureus* growth was little. Emodin played an important role in stage 2 of the growth curve of *S. aureus*, and aloe-emodin played an important role both in stage 1 and stage 2, especially in stage 1. The combination of emodin and aloe-emodin might play a double inhibitory role. Therefore, we chose the synergistic effect of emodin and aloe-emodin. When the growth rate constant k_1 of *S. aureus* was 50%k_0, the corresponding concentration of aloe-emodin was 6.4 μg.mL^{-1}. When the growth rate constant k_2 of *S. aureus* was 50%k_0, the corresponding concentration of emodin was 0.8 μg.mL^{-1}. We chose the half-inhibitory concentration of aloe-emodin and emodin as the combined dose. The results showed the following: (1) AE + E had the strongest bacteriostatic activity, followed by emodin, aloe-emodin and physcion, suggesting that the substituted positions and number of hydroxyls in the core structure of emodin might play important roles in the antibacterial effect. (2) The synergistic effect of two monomers was stronger than each monomer alone. (3) The synergistic effect of drugs could reduce dosage and thus toxicity, providing useful references for screening novel antibacterial drugs with high efficacy and low toxicity. (4) Compared to traditional microbiological techniques, noninvasive and nondestructive microcalorimetric investigations evaluating the antibacterial effects of drugs were more intuitive and convenient. (5) With the potential for automation at high sensitivity and high accuracy, microcalorimetry can provide real time, online and important dynamic information. Hence, microcalorimetry may become a popular method for examining the antimicrobial effects of drugs [41].

In addition, a common characteristic of herbal medicines is that all of the active ingredients function together for effective therapy that is greater than the individual compound [19, 20]. Based on this fact, we have analyzed the synergistic effects of several active monomers or constituents extracted from herbal medicines, avoiding interference from other inactive monomers and thereby reducing the total dosage, side effects and drug resistance. Such combined impacts might produce better effects than the herbal medicine. Although separation of active constituents or effective monomers was difficult, high-performance liquid chromatography and high-speed counter-current chromatography could be employed to extract and separate active monomers [21, 42–44]. Therefore, the synergistic effect of a few active monomers or constituents extracted from herbal medicines may become an effective strategy for studying antimicrobial effects. Combinations of active ingredients extracted from natural medicines are good choices for research of novel antibacterial agents with high efficacy and low toxicity and for reducing the prevalence of multidrug-resistant bacteria.

Conclusions

The anthraquinone derivatives (emodin, aloe-emodin and physcion) from Chinese Rhubarb had different inhibitory effect and different target on *S. aureus*. The inhibitory of physcion on *S. aureus* was little, far weaker than emodin and aloe-emodin. Emodin and physcion mainly played a role in stage 2 of the growth curve of *S. aureus*, and aloe-emodin played a role in stage 1 and stage 2. The combination of emodin and aloe-emodin played a role in stage 1 and stage 2 of the growth curve of *S. aureus* and had a stronger antibacterial activity than emodin and aloe-emodin alone. These results may provide reference for combination of active compounds.

Acknowledgements This study was supported by Research Project of Liaoning Provincial Department of Education (No. JYTFW201915). Xiangka Hu acknowledges their team for their help.

Compliance with ethical standards

Conflict of interest The authors declare no conflicts of interest.

References

1. Tong SY, Davis JS, Eichenberger E, Holland TL, Fowler VG Jr. Staphylococcus aureus infections: epidemiology, pathophysiology, clinical manifestations, and management. Clin Microbiol Rev. 2015;28:603–61.
2. Rd AF, Torres VJ. The bicomponent pore-forming leucocidins of Staphylococcus aureus. Microbiol Mol Biol Rev Mmbr. 2014;78:199–230.
3. Kong C, Neoh HM, Nathan S. Targeting staphylococcus aureus toxins: a potential form of anti-virulence therapy. Toxins. 2016. https://doi.org/10.3390/toxins8030072.
4. Kong WJ, Xing XY, Xiao XH, Zhao YL, Wei JH, Wang JB, et al. Effect of berberine on *Escherichia coli*, *Bacillus subtilis*, and their mixtures as determined by isothermal microcalorimetry. Appl Microbiol Biotechnol. 2012;96:503–10.
5. Liu J, Wu F, Chen C. Design and synthesis of aloe-emodin derivatives as potent anti-tyrosinase, antibacterial and anti-inflammatory agents. Bioorg Med Chem Lett. 2015;25:5142–6.
6. Zhu T, Zhang W, Feng SJ, Yu HP. Emodin suppresses LPS-induced inflammation in RAW264.7 cells through a PPARγ-dependent pathway. Int Immunopharmacol. 2016;34:16–24.
7. Shrimali D, Shanmugam MK, Kumar AP, Zhang J, Tan BK, Ahn KS, et al. Targeted abrogation of diverse signal transduction

cascades by emodin for the treatment of inflammatory disorders and cancer. Cancer Lett. 2013;341:139–49.
8. Xiong Y, Ren L, Wang Z, Hu Z, Zhou Y. Anti-proliferative effect of physcion on human gastric cell line via inducing ROS-dependent apoptosis. Cell Biochem Biophys. 2015. https://doi.org/10.1007/s12013-015-0674-9.
9. Acevedo-Duncan M, Russell C, Patel S, Patel R. Aloe–emodin modulates PKC isozymes, inhibits proliferation, and induces apoptosis in U-373MG glioma cells. Int Immunopharmacol. 2004;4:1775–84.
10. Pang M, Yang Z, Zhang X, Liu Z, Fan J, Zhang H. Physcion, a naturally occurring anthraquinone derivative, induces apoptosis and autophagy in human nasopharyngeal carcinoma. Acta Pharmacol Sin. 2016;37:1623–40.
11. Hu C, Dong T, Li R, Lu J, Wei X, Liu P. Emodin inhibits epithelial to mesenchymal transition in epithelial ovarian cancer cells by regulation of GSK-3β/β-catenin/ZEB1 signaling pathway. Oncol Rep. 2016;35:2027–34.
12. Zi-Qing H, Huang HQ, Tan HM, Liu PQ, Zhao LZ, Chen SR, et al. Emodin inhibits dietary induced atherosclerosis by antioxidation and regulation of the sphingomyelin pathway in rabbits. Chin Med J. 2006;119(10):868–70.
13. Li H, Wang X, Liu Y, Pan D, Wang Y, Yang N, et al. Hepatoprotection and hepatotoxicity of Heshouwu, a Chinese medicinal herb: context of the paradoxical effect. Food Chem Toxicol. 2016;108:407–18.
14. Liu H, Gu L, Tu Y, Hu H, Huang Y, Sun W. Emodin ameliorates cisplatin-induced apoptosis of rat renal tubular cells in vitro by activating autophagy. Acta Pharmacol Sin. 2016;37:235–45.
15. Basu S, Ghosh A, Hazra B. Evaluation of the antibacterial activity of *Ventilago madraspatana* Gaertn., *Rubia cordifolia* Linn. and *Lantana camara* Linn.: isolation of emodin and physcion as active antibacterial agents. Phytother Res. 2005;19:888–94.
16. Siri M, Ruocco MJF, Achilli E, Pizzuto M, Delgado JF, Ruysschaert JM, et al. Effect of structure in ionised albumin based nanoparticle: characterisation, Emodin interaction, and in vitro cytotoxicity. Mater Sci Eng C Mater Biol Appl. 2019. https://doi.org/10.1016/j.msec.2019.109813.
17. Yu Y, Liu H, Yang D, He F, Yuan Y, Guo J, et al. Aloe-emodin attenuates myocardial infarction and apoptosis via up-regulating miR-133 expression. Pharmacol Res. 2019. https://doi.org/10.1016/j.phrs.2019.104315.
18. Pan X, Wang C, Li Y, Zhu L, Zhang T. Protective autophagy induced by physcion suppresses hepatocellular carcinoma cell metastasis by inactivating the JAK2/STAT3 Axis. Life Sci. 2018;214:124–35.
19. Meng X, Zhou X, Wang T, Li F, Li H, Li J, et al. Microcalorimetric study on the activation effects of Salviae miltiorrhizae combined with Radix puerariae on mice splenic lymphocytes. J Therm Anal Calorim. 2019;137:841–8.
20. Wang T, Zhou X, Zou W, Zhang P, Wang J, Li H, et al. Synergistic effects of Ginseng C. A. Mey and Astragalus membranaceus (Fisch.) Bunge on activating mice splenic lymphocytes detected by microcalorimetry and the underlying mechanisms predicted by in silico network analysis. J Therm Anal Calorim. 2018;132:1933–42.
21. Yan D, Li J, Xiong Y, Zhang C, Luo J, Han Y, Wang R, Jin C, Qian H, Li J, Qiu L, Peng C, Lin Y, Song X, Xiao X. Promotion of quality standard of herbal medicine by constituent removing and adding. Sci Rep. 2014. https://doi.org/10.1038/srep03668.
22. Tafin UF, Clauss M, Meis JF, Trampuz A, Hauser PM, Bille J. Isothermal microcalorimetry: a novel method for real-time determination of antifungal susceptibility of Aspergillus species. Clin Microbiol Infect. 2012;18:241–5.
23. von Ah U, Wirz D, Daniels AU. Isothermal micro calorimetry—a new method for MIC determinations: results for 12 antibiotics and reference strains of *E. coli* and *S. aureus*. BMC Microbiol. 2009. https://doi.org/10.1186/1471-2180-9-106.
24. Kong W, Wang J, Xing X, Xiao X, Zhao Y, Zang Q, et al. Antifungal evaluation of cholic acid and its derivatives on *Candida albicans* by microcalorimetry and chemometrics. Anal Chim Acta. 2011;689:250–6.
25. Chihara T, Shimpo K, Beppu H, Yamamoto N, Kaneko T, Wakamatsu K, et al. Effects of aloe-emodin and emodin on proliferation of the MKN45 human gastric cancer cell line. Asian Pac J Cancer Prev APJCP. 2015;16:3887–91.
26. Ding Z, Xu F, Tang J, Li G, Jiang P, Tang Z, et al. Physcion 8-O-β-glucopyranoside prevents hypoxia-induced epithelial-mesenchymal transition in colorectal cancer HCT116 cells by modulating EMMPRIN. Neoplasma. 2016;63:351–61.
27. Kong WJ, Wang JB, Zang QC, Jin C, Wang ZW, Xing XY, et al. A novel "target constituent knock-out" strategy coupled with TLC, UPLC–ELSD and microcalorimetry for preliminary screening of antibacterial constituents in Calculus bovis. J Chromatogr B. 2011;879:3565–73.
28. Wadsö I. Isothermal microcalorimetry in applied biology. Thermochim Acta. 2002;394:305–11.
29. Kong W, Wang J, Xiao X, Chen S, Yang M. Evaluation of antibacterial effect and mode of Coptidis rhizoma by microcalorimetry coupled with chemometric techniques. Analyst. 2012;137:216–22.
30. Ma Z-j, Zhang C-e, Wang R-l, Zang Q-c, Yu X-h, Wang J-B, et al. Microcalorimetry combined with chemometics for antibacterial evaluation of Sophora alopecuroides on Staphylococcus aureus. J Therm Anal Calorim. 2018;134:1883–91.
31. Yi ZB, Yan Y, Liang YZ, Bao Z. Evaluation of the antimicrobial mode of berberine by LC/ESI-MS combined with principal component analysis. J Pharm Biomed Anal. 2007;44:301–4.
32. Yi LZ, Yuan DL, Liang YZ, Xie PS, Zhao Y. Quality control and discrimination of pericarpium citri reticulatae and pericarpium citri reticulatae viride based on high-performance liquid chromatographic fingerprints and multivariate statistical analysis. Anal Chim Acta. 2007;588:207–15.
33. Chen Y, Zhu SB, Xie MY, Nie SP, Liu W, Li C, et al. Quality control and original discrimination of *Ganoderma lucidum* based on high-performance liquid chromatographic fingerprints and combined chemometrics methods. Anal Chim Acta. 2008;623:146–56.
34. Kong WJ, Wang JB, Jin C, Zhao YL, Dai CM, Xiao XH, et al. Effect of emodin on *Candida albicans* growth investigated by microcalorimetry combined with chemometric analysis. Appl Microbiol Biotechnol. 2009;83:1183–90.
35. Fan DL, Xiao XH, Ma XJ. Calorimetric study of the effect of protoberberine alkaloids in *Coptis chinensis* Franch on *Staphylococcus aureus* growth. Thermochim Acta. 2008;480:49–52.
36. Kong W, Zhao Y, Shan L, Xiao X, Guo W. Thermochemical studies on the quantity-antibacterial effect relationship of four organic acids from Radix Isatidis on *Escherichia coli* growth. Biol Pharmaceut Bull. 2008;31:1301–5.
37. Brown AF, Murphy AG, Lalor SJ, Leech JM, O'Keeffe KM, Aogáin MM, et al. Memory Th1 cells are protective in invasive *Staphylococcus aureus* infection. PLoS Pathog. 2015. https://doi.org/10.1371/journal.ppat.1005226.
38. Schmidt T, Kock MM, Ehlers MM. Molecular characterization of staphylococcus aureus isolated from bovine mastitis and close human contacts in south african dairy herds: genetic diversity and inter-species host transmission. Front Microbiol. 2017. https://doi.org/10.3389/fmicb.2017.00511.

39. Bröker BM, Daniel M, Vincent P. The T cell response to *Staphylococcus aureus*. Pathogens. 2016. https://doi.org/10.3390/pathogens5010031.
40. Wang Z, Xue R, Cui J, Wang J, Fan W, Zhang H, et al. Antibacterial activity of a polysaccharide produced from *Chaetomium globosum* CGMCC 6882. Int J Biol Macromol. 2019;125:376–82.
41. Li X, Jiang J-H, Gu H-W, Wei D-L, Li C-H, Li X, et al. Synthesis and biothermokinetic study of a new Schiff base and its bismuth(III) complex on the growth metabolism of *S. pombe* and *H. pylori* cell lines. J Therm Anal Calorim. 2018;132:1913–22.
42. Wei Y, Xie Q, Dong W, Ito Y. Separation of epigallocatechin and flavonoids from *Hypericum perforatum* L. by high-speed counter-current chromatography and preparative high-performance liquid chromatography. J Chromatogr A. 2009;1216:4313–8.
43. Guo YX, Zhou LL, Li T, Wang LH. Preparative separation of lithospermic acid B from *Salvia miltiorrhiza* by polyamide resin and preparative high-performance liquid chromatography. J Chromatogr A. 2011;1218:4606–11.
44. Huang XY, Fu JF, Di DL. Preparative isolation and purification of steviol glycosides from *Stevia rebaudiana* Bertoni using high-speed counter-current chromatography. Sep Purif Technol. 2010;71:220–4.